

ENERGY-DEPENDENT GRB PULSE WIDTH DUE TO THE CURVATURE EFFECT AND INTRINSIC BAND SPECTRUM

Z. Y. Peng^{1,2}, X. H. Zhao^{2,3}, Y. Yin⁴, Y. Y. Bao⁵, L. Ma^{1,6}

Received _____; accepted _____

¹Department of Physics, Yunnan Normal University, Kunming 650092, China;
pzy@ynao.ac.cn

²Key Laboratory for the Structure and Evolution of Celestial Objects, Chinese Academy of Sciences, Kunming 650011, China

³National Astronomical Observatories/Yunnan Observatory, Chinese Academy of Sciences, P. O. Box 110, Kunming 650011, China

⁴Department of Physics, Liupanshui Normal College, Liupanshui 553004, China

⁵Department of Physics, Yuxi Normal College, Yuxi 653100, China

⁶Author to whom correspondence should be addressed

ABSTRACT

Previous studies have found that the width of gamma-ray burst (GRB) pulse is energy dependent and that it decreases as a power-law function with increasing photon energy. In this work we have investigated the relation between the energy dependence of pulse and the so-called Band spectrum by using a sample including 51 well-separated fast rise and exponential decay long-duration GRB pulses observed by BATSE (Burst and Transient Source Experiment on the Compton Gamma Ray Observatory). We first decompose these pulses into rise, and decay phases and find the rise widths, and the decay widths also behavior as a power-law function with photon energy. Then we investigate statistically the relations between the three power-law indices of the rise, decay and total width of pulse (denoted as δ_r , δ_d and δ_w , respectively) and the three Band spectral parameters, high-energy index (α), low-energy index (β) and peak energy (E_p). It is found that (1) α is strongly correlated with δ_w and δ_d but seems uncorrelated with δ_r ; (2) β is weakly correlated with the three power-law indices and (3) E_p does not show evident correlations with the three power-law indices. We further investigate the origin of $\delta_d - \alpha$ and $\delta_w - \alpha$. We show that the curvature effect and the intrinsic Band spectrum could naturally lead to the energy dependence of GRB pulse width and also the $\delta_d - \alpha$ and $\delta_w - \alpha$ correlations. Our results would hold so long as the shell emitting gamma rays has a curve surface and the intrinsic spectrum is a Band spectrum or broken power law. The strong $\delta_d - \alpha$ correlation and inapparent correlations between δ_r and three Band spectral parameters also suggest that the rise and decay phases of GRB pulses have different origins.

Subject headings: gamma rays: bursts — method: statistical

1. INTRODUCTION

The origin of the gamma-ray bursts (GRBs) still remains unclear though it has been found for more than 40 years and many progresses have been made. Generally GRBs have complex temporal profiles with plenty of pulses and pulse is the basic element of light curves. The pulses for most bursts overlap each other, while there also exist well-separated pulses within some bursts. A lot of statistical studies about pulses have been made because they can provide us valuable clues to the radiation mechanism and underlying processes of GRB. In early statistical analysis, the width of GRB pulses was found to be energy dependent, i.e., the higher energies, the narrower widths (e.g., Link, Epstein & Friedhorsky 1993). Using the average autocorrelation function to study the average pulse width, Fenimore et al. (1995) showed that the average pulse width of many bursts dependence on energy is well fitted by a power-law function with the power-law index about -0.4. The result was confirmed by later studies (e.g., Norris et al. 1996; Norris, Marani & Bonnell 2000; Nemiroff 2000; Crew et al. 2003; Norris et al. 2005). Peng et al. (2006) employed two samples consisting of 82 well-separated pulses to test the relation and found a power-law anti-correlation between the full pulse width and energy. A power-law correlation between the pulse width ratio and energy is also seen in the light curves of the majority of bursts in the two samples within the energy range of BATSE (Burst and Transient Source Experiment on the Compton Gamma Ray Observatory). Recently it is found that this power-law relation can be extended to X-ray bands (see, Zhang & Qin 2008, Zhang 2008) as well as X-ray flare (Chincarini et al. 2010). In addition, Zhang & Qin (2007) showed that the pulse peak time, the rise time scale, and the decay time scale on energy are also power-law functions.

The origin of the dependence of the pulse width on photon energy is still unclear to date. It has been suggested that the power-law relation could be attributed to synchrotron

cooling (e.g., Kazanas, Titarchuk & Hua 1998, Chiang 1998; Dermer 1998; Wang et al. 2000), which gives a slope of $-1/2$ between the pulse width and photon energy, similar to the observed -0.4 . However, the synchrotron cooling is unlikely to be responsible for the relation due to its too short timescale relative to the pulse width. Under the assumption that the Doppler effect of the relativistically expanding fireball surface (or, in some papers, the curvature effect) is important, Qin et al. (2005) showed that, in most cases, this power-law relationship would exist in a certain energy range, and, within a similar range, a power-law relation of an opposite trend between the ratio of the rising width to the decaying width and energy would be expected for the same burst. Shen, Song & Li (2005) also considered the curvature effect and found the slope of the power-law relation to be $-0.1\sim-0.2$, less than the observed -0.4 . These suggest that the curvature effect is an important factor to form the relation.

The observed spectrum of GRB is usually a broken power-law form. The smooth connection of two power laws is the so-called Band function, which can describe well the observed spectrum (Band et al. 1993). Three parameters in the Band function are used to characterize the spectral shape: the low-energy power-law index α , the high-energy power-law index β , and the peak of the spectral energy distribution E_p . It is found that the distributions of the power-law slopes of pulse width and photon energy obtained by Peng et al. (2006) and Zhang & Qin (2007) have large dispersions for different bursts, while the GRB spectra also vary dramatically for two different bursts. Whether the energy dependence of pulse is connected with the observed spectrum in some way or not? If it is true, then what does it imply for the mechanism of energy dependence of GRB pulse and whether does it supply some useful clues to the origin of the pulse rise and the decay phase? These motivate our investigations below. In Section 2, we present the sample description and pulse modeling. The analysis results are given in Section 3. We give the possible implications of the statistical correlations in Section 4. Conclusions and discussion are

presented in the last section.

2. SAMPLE DESCRIPTION AND PULSE MODELING

The sample we selected comes from Peng et al. (2010) observed by CGRO/BATSE with durations longer than 2 s, which contains 52 individual FRED pulses with the peak fluxes are greater than $1.0 \text{ photon cm}^{-2} \text{ s}^{-1}$ on a 256-ms time-scale (for further information about the sample selection and spectral analysis, see Kocevski et al. 2003; Peng et al. 2009a; Peng et al. 2010).

In order to investigate the pulse temporal properties, we must model these pulses with a pulse model. A form proportional to the inverse of the product of two exponentials, one increasing and one decreasing with time, derived by Norris et al. (2005), is a good model to describe the GRB pulses. Thus we select the pulse model to model our selected pulses, which can be rewritten as

$$I(t) = A\lambda \exp[-\tau_1/(t - t_s) - (t - t_s)/\tau_2], \quad (1)$$

where t is the time since trigger, A is the pulse amplitude, t_s is the pulse start time, τ_1 and τ_2 are the characteristics of the pulse rise and the pulse decay, and $\lambda = \exp[2(\tau_1/\tau_2)]^{1/2}$.

Similar to Peng et al. (2006, 2009a) and Hakkila et al. (2008) we use the nonlinear least squares routine MPFIT and develop and apply an interactive IDL routine to fit all of the pulses, which allows the user to set and adjust the initial pulse parameters manually before allowing the fitting routine to converge on the best-fitting model via the reduced χ^2 minimization. For each burst we require that the signal should be detectable in at least three channels (in this way, the relationship between the pulse width and energy can be studied). The fits are examined many times to ensure that they are indeed the best ones.

We demonstrate the results with the fitting to GRB 950624b (BATSE trigger 3648),

in which three well-separated pulses were observed in four BATSE energy channels. The narrow distribution of the fitting χ^2 values per degree of freedom (see, the right panel in Figure 1) indicates that the two-exponential model is sufficient to model the pulse light curves.

The parameter values for all identified pulses are obtained, including the pulse peak intensity (A), pulse onset time (t_s), effective onset time (t_{eff}), and peak time (T_{peak}), as well as the two fundamental timescales (τ_1 and τ_2) (see Table 2 in Norris et al. 2005). The effective onset time, t_{eff} , is defined as the time when the pulse reaches 0.01 times of the peak intensity. Both onset times are relative to the burst trigger time. According to the fitting parameters we can obtain the measured pulse temporal properties including the pulse width $w = \Delta\tau_{1/e} = \tau_2(1 + 2 \ln \lambda)^{1/2}$, the pulse rise width, $\tau_{rise} = \frac{1}{2}w(1 - k)$, and the decay width $\tau_{decay} = \frac{1}{2}w(1 + k)$. Fitting the pulse width, the pulse rise width, the pulse decay width (in the logarithm) per channel as a function of the geometric means of the lower and upper BATSE channel boundaries (using 300–1000 keV for channel 4) (Norris et al. 2005) shows the power-law relations indeed exist and the power-law indices are thus obtained (let δ_w , δ_r , and δ_d denote the indices of the power-law relations between w , τ_{rise} , and τ_{decay} and energy, respectively). Therefore, the dependence of the three time quantities on energy can be parameterized by the power-law index. Example plots of the relations between the temporal properties and energy are illustrated in Figure 2 and the three power-law indices are presented in Table 1.

In order to obtain the consistent time intervals between the light curves and spectra in the same pulse the time-integrated spectra are reanalyzed for each pulse of our sample based on the analysis of Peng et al. (2009a), which provided a detailed data description and spectral modeling of our sample. Only the so-called Band model (Band et al. 1993) is used to model the pulse spectra in this work. In the end there are 51 pulses that are included in

our analysis after removing one bad pulse spectrum with Band model in the certain time interval. The three spectral parameters for all of the pulses are also listed in Table 1.

Table 1. A List of the Burst Sample and Various Parameters.

Trigger	δ_w	δ_r	δ_d	α	β	E_p (keV)
563	-0.694 ± 0.008	-0.566 ± 0.042	-0.729 ± 0.019	-0.481 ± 0.082	-2.669 ± 0.145	184.500 ± 7.450
907	-0.542 ± 0.016	-0.270 ± 0.049	-0.647 ± 0.023	-0.188 ± 0.065	-2.869 ± 0.130	188.400 ± 4.740
914	-0.353 ± 0.039	-0.408 ± 0.080	-0.323 ± 0.020	-0.848 ± 0.191	-2.475 ± 0.114	100.900 ± 6.990
973_1	-0.176 ± 0.007	-0.170 ± 0.009	-0.178 ± 0.006	-1.102 ± 0.024	-2.084 ± 0.034	298.500 ± 12.700
973_2	-0.230 ± 0.019	-0.176 ± 0.016	-0.256 ± 0.024	-1.431 ± 0.044	-2.264 ± 0.130	254.500 ± 25.600
999	-0.250 ± 0.028	-0.108 ± 0.047	-0.307 ± 0.023	-0.971 ± 0.052	-2.010 ± 0.067	388.800 ± 36.500
1406	-0.379 ± 0.072	-0.466 ± 0.082	-0.352 ± 0.069	-0.616 ± 0.127	-2.138 ± 0.033	121.700 ± 6.620
1883	-0.207 ± 0.062	-0.165 ± 0.047	-0.230 ± 0.070	-1.294 ± 0.039	-3.772 ± 0.850	291.000 ± 19.000
1956	-0.163 ± 0.005	-0.079 ± 0.008	-0.215 ± 0.014	-1.132 ± 0.093	-2.385 ± 0.117	144.300 ± 10.300
2083	-0.406 ± 0.010	-0.278 ± 0.045	-0.437 ± 0.024	-1.326 ± 0.039	-3.533 ± 0.191	74.380 ± 1.180
2138	-0.408 ± 0.083	-0.240 ± 0.010	-0.474 ± 0.111	-0.315 ± 0.151	-2.933 ± 0.408	222.900 ± 14.800
2193	-0.582 ± 0.033	-0.374 ± 0.025	-0.571 ± 0.012	0.384 ± 0.064	-2.898 ± 0.155	274.000 ± 6.480
2387	-0.224 ± 0.009	-0.143 ± 0.017	-0.261 ± 0.020	-0.372 ± 0.048	-2.482 ± 0.049	158.400 ± 3.200
2484	-0.337 ± 0.010	-0.199 ± 0.016	-0.407 ± 0.022	-0.310 ± 0.123	-3.287 ± 0.549	178.100 ± 8.220
2662	-0.490 ± 0.019	-0.370 ± 0.031	-0.544 ± 0.016	-0.700 ± 0.129	-2.838 ± 0.383	178.800 ± 12.500
2665	-0.799 ± 0.128	-0.583 ± 0.075	-0.890 ± 0.146	0.292 ± 0.271	-2.856 ± 0.137	87.720 ± 3.310
2700	-0.223 ± 0.011	-0.534 ± 0.006	-0.108 ± 0.012	-1.361 ± 0.044	-3.005 ± 0.614	249.800 ± 16.300
2880	-0.426 ± 0.002	-0.269 ± 0.082	-0.462 ± 0.021	-0.659 ± 0.132	-3.114 ± 0.406	134.500 ± 6.410
2919	-0.274 ± 0.041	-0.222 ± 0.180	-0.296 ± 0.025	-1.166 ± 0.057	-2.253 ± 0.146	289.000 ± 28.500
3003	-0.095 ± 0.014	-0.058 ± 0.027	-0.112 ± 0.009	-1.122 ± 0.034	-2.053 ± 0.099	489.600 ± 47.900
3143	-0.288 ± 0.009	-0.147 ± 0.038	-0.351 ± 0.030	-0.916 ± 0.500	-2.032 ± 0.077	101.700 ± 26.500
3256	-0.613 ± 0.003	-0.653 ± 0.027	-0.598 ± 0.006	-0.028 ± 0.162	-2.939 ± 0.236	145.800 ± 6.190
3257	-0.578 ± 0.036	-0.449 ± 0.030	-0.613 ± 0.039	-0.231 ± 0.065	-3.040 ± 0.226	195.900 ± 5.160
3415	-0.193 ± 0.021	-0.041 ± 0.013	-0.254 ± 0.034	-1.000 ± 0.158	-2.093 ± 0.103	182.500 ± 27.000
3648_2	-0.528 ± 0.012	-0.626 ± 0.060	-0.479 ± 0.013	-0.862 ± 0.333	-2.232 ± 0.064	98.210 ± 10.000
3648_3	-0.528 ± 0.031	-0.273 ± 0.027	-0.625 ± 0.028	-0.748 ± 0.052	-2.802 ± 0.155	217.200 ± 7.180
3765	-0.231 ± 0.038	-0.257 ± 0.165	-0.227 ± 0.015	-0.872 ± 0.022	-2.733 ± 0.101	308.800 ± 7.750
3875	-0.425 ± 0.024	-0.280 ± 0.142	-0.464 ± 0.063	-1.245 ± 0.333	-2.974 ± 0.219	56.380 ± 6.090
3954	-0.117 ± 0.013	-0.253 ± 0.022	-0.064 ± 0.023	-1.153 ± 0.059	-1.927 ± 0.049	295.500 ± 32.100
4350	-0.136 ± 0.052	-0.389 ± 0.159	-0.047 ± 0.012	-1.467 ± 0.105	-2.357 ± 0.420	263.500 ± 62.500
5478	-0.427 ± 0.006	-0.225 ± 0.117	-0.496 ± 0.033	-0.287 ± 0.107	-2.896 ± 0.265	158.100 ± 6.410
5517	-0.288 ± 0.070	-0.230 ± 0.026	-0.321 ± 0.094	-1.156 ± 0.154	-2.667 ± 0.000	149.700 ± 14.500

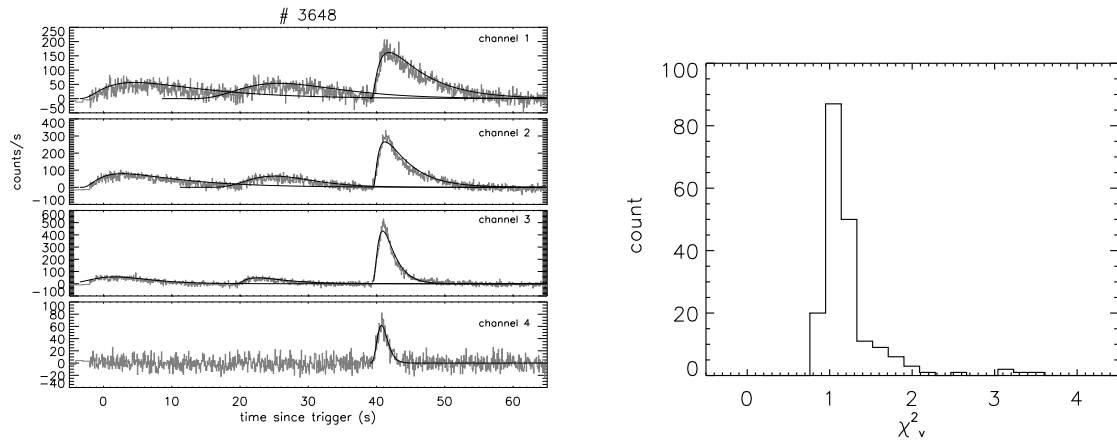


Fig. 1.— Example plots of GRB 950624b pulse fits for BATSE channels (left panel) and the histogram of χ^2 in our sample (right panel).

3. ANALYSIS RESULTS

3.1. THE RELATIONS AMONG THE POWER-LAW INDICES

Employing a sample consisting of 24 long-lag pulses Zhang & Qin (2007) studied the relations between the pulse temporal properties (width, rise width, decay width and peak time) and energy and found the pulse temporal properties are power-law functions of energy. In this section, we recheck the relations for the following two reasons. Firstly, the sample we used is much larger than that of Zhang & Qin (2007). Secondly, the FRED bursts are temporally and spectrally distinguished from long-lag bursts (Peng et al. 2010).

Displayed in Figure 3 are the histograms of the three indices. The distribution parameters are listed in Table 2. From Figure 3 and Table 2 we find the distributions of these indices share the similar distribution width but they have large dispersions. The large dispersions imply that the energy dependence of the temporal properties may not be the same for different bursts. In addition, it is found that most of the power-law indices are much smaller than those of long-lag pulse derived by Zhang & Qin (2007).

We also examine the relationships between the power-law indices of the temporal properties on energy. Figure 4 shows the relationships between them. The Spearman rank-order correlation analysis of the three quantities are listed in Table 3. The straight lines are fitted to the points: (1) $\delta_r = (0.11 \pm 0.01) + (1.31 \pm 0.03) \delta_w$; (2) $\delta_d = (-0.07 \pm 0.06) + (1.01 \pm 0.02) \delta_w$; (3) $\delta_r = (0.09 \pm 0.01) + (1.25 \pm 0.03) \delta_d$. It is found that the δ_d is strongly correlated with δ_w and the slope between them is close to 1. And so the two indices may be viewed as mutual surrogates. While the other two index pairs are obviously less correlated, which strongly indicates that the temporal properties (rise and the decay times) of the pulses do not evolve independently from each other, instead, their evolution is tightly coupled.

Table 1—Continued

Trigger	δ_w	δ_r	δ_d	α	β	E_p (keV)
5523	-0.269 ± 0.009	-0.231 ± 0.018	-0.290 ± 0.004	-1.266 ± 0.173	-2.382 ± 0.188	129.200 ± 15.900
5601	-0.335 ± 0.024	-0.246 ± 0.041	-0.380 ± 0.030	-0.725 ± 0.057	-2.295 ± 0.076	223.200 ± 10.300
6159	-0.155 ± 0.041	0.035 ± 0.008	-0.237 ± 0.052	-0.907 ± 0.446	-2.260 ± 0.039	73.200 ± 8.610
6397	-0.215 ± 0.008	-0.116 ± 0.014	-0.259 ± 0.017	-0.648 ± 0.042	-2.572 ± 0.104	192.500 ± 5.440
6504	-0.634 ± 0.037	-0.475 ± 0.005	-0.687 ± 0.049	0.067 ± 0.099	-2.729 ± 0.156	157.200 ± 4.970
6621	-0.112 ± 0.013	-0.074 ± 0.035	-0.126 ± 0.009	-1.086 ± 0.074	-2.424 ± 0.079	128.900 ± 5.960
6625	-0.304 ± 0.001	-0.253 ± 0.009	-0.331 ± 0.006	-0.873 ± 0.120	-2.841 ± 0.124	76.900 ± 2.000
6657	-0.571 ± 0.051	-1.017 ± 0.258	-0.521 ± 0.058	-1.043 ± 0.420	-2.334 ± 0.159	95.180 ± 13.100
6930	-0.264 ± 0.016	-0.171 ± 0.021	-0.314 ± 0.012	-0.639 ± 0.131	-2.294 ± 0.046	95.180 ± 4.340
7293	-0.495 ± 0.014	-0.281 ± 0.062	-0.585 ± 0.039	0.313 ± 0.089	-2.979 ± 0.120	161.300 ± 3.460
7295	-0.410 ± 0.013	-0.319 ± 0.020	-0.443 ± 0.022	0.404 ± 0.094	-2.628 ± 0.180	373.500 ± 16.500
7475	-0.109 ± 0.010	-0.141 ± 0.012	-0.092 ± 0.010	-1.315 ± 0.066	-1.979 ± 0.029	149.900 ± 14.300
7548	-0.227 ± 0.001	-0.296 ± 0.051	-0.195 ± 0.026	-0.836 ± 0.104	-2.250 ± 0.000	176.800 ± 11.100
7588	-0.210 ± 0.024	-0.423 ± 0.026	-0.134 ± 0.027	-0.729 ± 0.208	-2.710 ± 0.097	71.290 ± 2.100
7638	-0.486 ± 0.012	-0.517 ± 0.010	-0.480 ± 0.013	-1.298 ± 0.389	-2.576 ± 0.090	54.170 ± 5.300
7648	-0.690 ± 0.197	-0.826 ± 0.292	-0.647 ± 0.162	-0.588 ± 0.100	-2.356 ± 0.000	201.100 ± 10.300
7711	-0.272 ± 0.031	-0.400 ± 0.025	-0.219 ± 0.032	-1.241 ± 0.051	-3.124 ± 0.806	211.200 ± 12.800
8049_1	-0.208 ± 0.003	-0.289 ± 0.034	-0.156 ± 0.018	-0.391 ± 0.104	-3.826 ± 0.550	164.300 ± 6.330
8049_2	-0.324 ± 0.032	-0.430 ± 0.012	-0.252 ± 0.063	-1.408 ± 0.072	-3.096 ± 0.410	157.400 ± 12.100

Table 2. A List of the Distribution Parameters of the Three Power-law Indices.

Power-law indices	Mean	Median	σ (modeled with a Gaussian profile)
δ_w	-0.35	-0.31	-0.32 ± 0.17
δ_r	-0.31	-0.27	-0.27 ± 0.17
δ_d	-0.37	-0.32	-0.33 ± 0.23

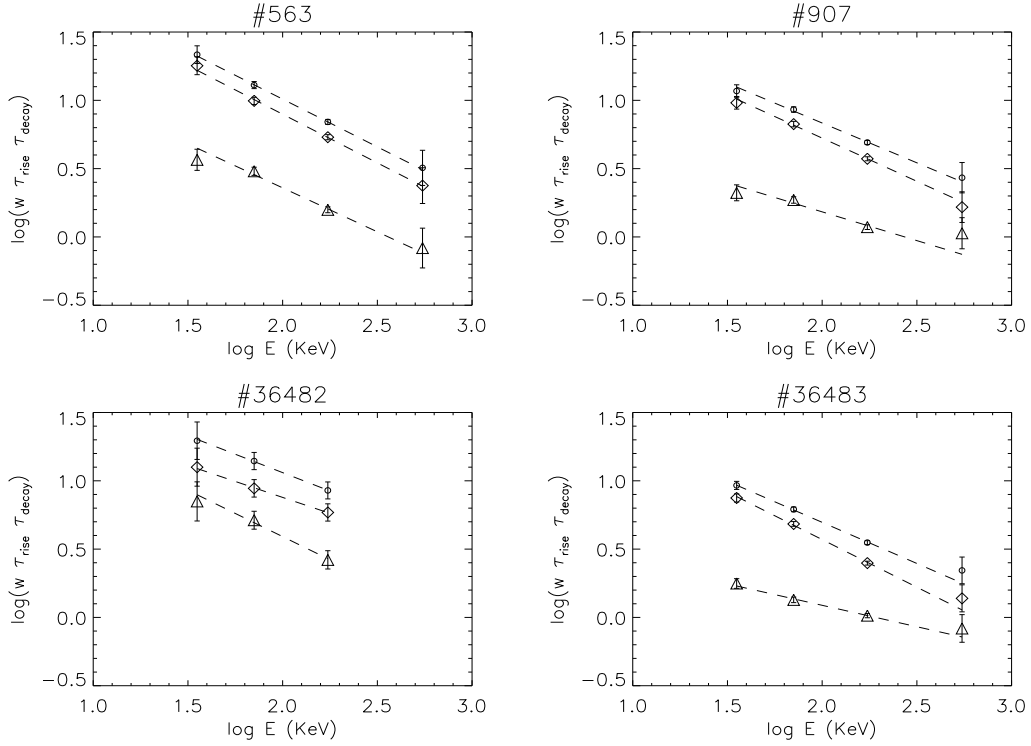


Fig. 2.— Example plots of the relations between the observed pulse temporal properties and energy for our selected samples, where the open circle, the diamond, the triangle and the square represent the pulse width, the pulse rise width, the pulse decay width, respectively. The power-law relations between them are evident.

Table 3. Correlations of the power-law index pairs.

Power-law indices	R_S	P_S
δ_w - δ_r	0.69	2.63×10^{-8}
δ_w - δ_d	0.96	2.93×10^{-28}
δ_r - δ_d	0.49	2.84×10^{-4}

Note. — R_S and P_S denote the Spearman rank-order correlation coefficient and significance, respectively.

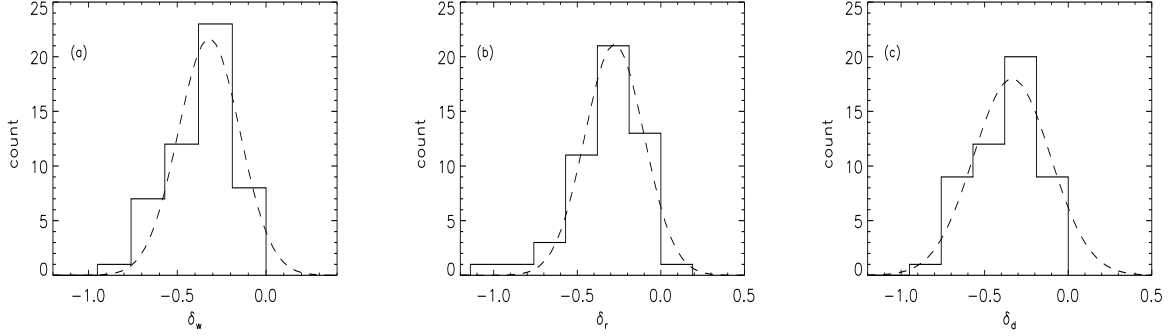


Fig. 3.— Histograms of the power-law indices δ_w (a), δ_r (b), and δ_d (c) obtained by fitting the pulse width, rise width, and decay width and energy with power-law functions, respectively. The dashed lines are the best fits by the Gaussian functions.

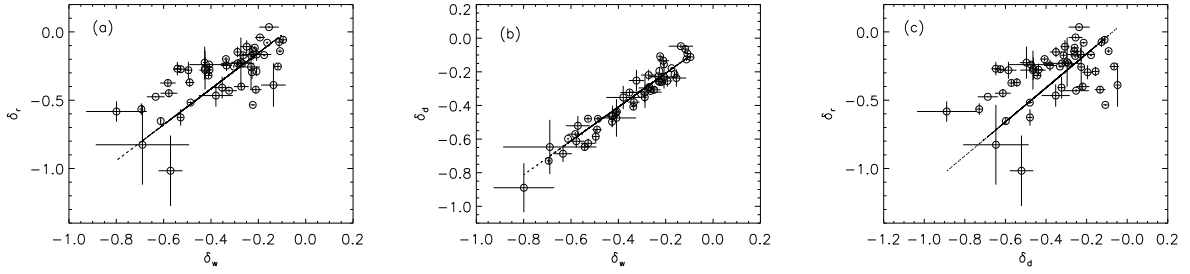


Fig. 4.— Relationships of the three power-law indices δ_r vs. δ_w (a), δ_d vs. δ_w (b), δ_r vs. δ_d (c). The dashed lines are the regression lines.

Table 4. Correlations of the Three Power-law Indices versus Spectral Parameters

Parameter	R_S	P_S	Parameter	R_S	P_S	Parameter	R_S	P_S
$\delta_w-\alpha$	-0.57	1.41×10^{-5}	$\delta_w-\beta$	0.39	4.42×10^{-3}	δ_w-E_p	0.20	1.05×10^{-1}
$\delta_r-\alpha$	-0.24	8.99×10^{-2}	$\delta_r-\beta$	0.34	1.37×10^{-2}	δ_r-E_p	0.19	1.77×10^{-1}
$\delta_d-\alpha$	-0.62	1.04×10^{-6}	$\delta_d-\beta$	0.32	2.22×10^{-2}	δ_d-E_p	0.21	1.44×10^{-1}

Note. — R_S and P_S denote the Spearman rank-order correlation coefficient and significance, respectively.

3.2. THE RELATIONS AMONG THE POWER-LAW INDICES AND THE BAND SPECTRAL PARAMETERS

Since the power-law indices reflect the spectral evolution of GRB pulse we wonder whether they are related to the spectral parameters or not. With the temporal and spectral parameters obtained in the previous section, we can examine the relationships between the power-law indices and the spectral shape parameters, low-energy index α , high-energy index β , and peak energy E_p . Illustrated in Figure 5 are the scatter plots of the power-law indices versus α . The Spearman rank-order correlation parameters are listed in Table 4. The regression analysis gives the best-fitting lines: (1) $\delta_w = (-0.63 \pm 0.01) + (0.40 \pm 0.01)\alpha$; (2) $\delta_r = (-0.70 \pm 0.02) + (0.50 \pm 0.02)\alpha$; (3) $\delta_d = (-0.62 \pm 0.01) + (0.39 \pm 0.01)\alpha$.

The strong anticorrelated relations are identified between δ_d and α as well as δ_w and α . However, there seem no correlation between δ_r and α and the dispersion is much larger than the other two parameter pairs. In addition, the slope and intercept of δ_r and α has apparent difference compared with that of δ_d and α . A possible interpretation of the phenomenon is that the mechanism causing the dependence of the rise width on energy might be different from the other temporal properties on energy. Another possible reason is that the mechanism of producing the rise phase is different from that of the decay phase.

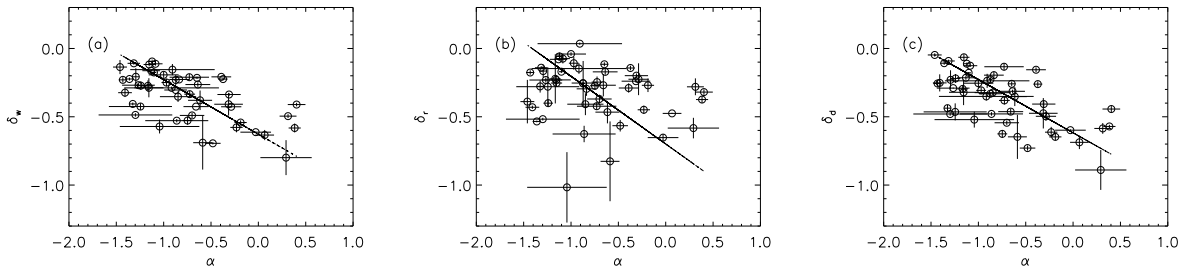


Fig. 5.— Power-law indices δ_w (a), δ_r (b) and δ_d (c) vs. low-energy power-law index α . The dashed lines are the best fitting lines.

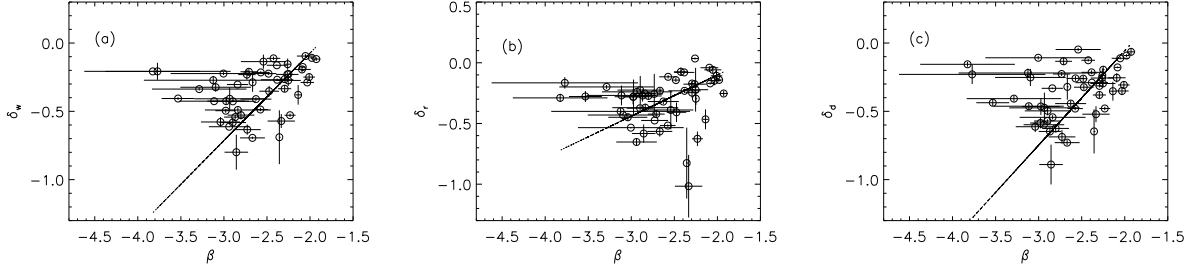


Fig. 6.— Power-law indices δ_w (a), δ_r (b), and δ_d (c) vs. high-energy power-law index β . The dashed lines are the best fitting lines.

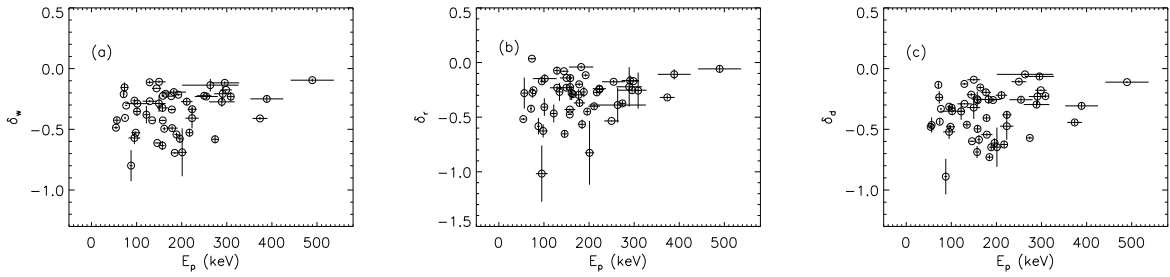


Fig. 7.— Power-law indices δ_w (a), δ_r (b), and δ_d (c) vs. peak energy E_p . No correlation is apparent.

Examining of the power-law indices versus the other two shaped parameters β and E_p , shows that all of the power-law indices are weakly correlated with the β (see, Figure 6 and Table 4). However, no apparent correlations are found between the three power-law indices and E_p (see, Figure 7 and Table 4).

4. IMPLICATIONS OF THE STATISTICAL CORRELATIONS

The origin of the found correlations between the power-law indices and the Band-spectrum parameters could be related to the GRB pulse formation mechanism. The mechanisms of the rise phase and decay phase of the pulse are different. The rise phase of the pulse is believed to be related to gamma-ray active time of emission region, while the decay phase originates from the curvature effect. The found strong $\delta_d - \alpha$ correlation and weak $\delta_r - \alpha$ correlation also suggest the different origins of the rise phase and decay phase. It is interesting to speculate the physical origin of the strong $\delta_d - \alpha$ correlation. Since δ_d is a quantity describing the decay phase, we consider the effect of the curvature effect on the energy dependence of the pulse.

4.1. The energy dependent of pulse width due to the curvature effect

In order to study the energy dependent of pulse width due to the curvature effect, we first calculate the decay profile of a pulse from a thin spherical surface expanding with relativistic speed. Define an emissivity

$$j'_{E'} = \sum'_{E'} \delta(t' - t'_0) \delta(R' - R'_0), \quad (2)$$

where $\sum'_{E'}$ is the surface brightness per unit photon energy interval in the comoving frame. Since the observed GRB spectrum is broken power law form, it is not unreasonable to

assume $\sum'_{E'}$ to be the following form:

$$\sum'_{E'} = \sum'_0 \begin{cases} (E'/E_p)^{1+\alpha} & E' < E'_p \\ (E'/E_p)^{1+\beta} & E' > E'_p \end{cases}, \quad (3)$$

where \sum'_0 is the normalized coefficient, E'_p is the intrinsic cutoff energy (comoving frame), and α and β are the low and high energy photon number spectrum slopes, respectively. As we know, more generally GRB spectrum is described by the so-called Band function:

$$\sum'_{E'} = \sum'_0 \begin{cases} \left(\frac{E'}{100\text{keV}}\right)^{1+\alpha} \exp\left[-\frac{E'(2+\alpha)}{E'_p}\right] & E' < E'_p(\alpha - \beta)/(2 + \alpha) \\ \left[\frac{(\alpha-\beta)E'_p}{(2+\alpha)100\text{keV}}\right]^{\alpha-\beta} \exp(\beta - \alpha)\left(\frac{E'}{100\text{keV}}\right)^{1+\beta} & E' > E'_p(\alpha - \beta)/(2 + \alpha) \end{cases}. \quad (4)$$

However we will find below, the broken power law spectra gives more explicit physical meaning than the Band function.

The observed photon flux density can be given by

$$F_E = \frac{1}{4\pi D_L^2} \int j_E dV = \frac{1}{2D_L^2} \iint j'_{E'} D^2 R^2 dR d\mu, \quad (5)$$

Here $D = 1/[\Gamma(1 - \beta_\Gamma\mu)]$ is the Doppler factor and the transformations $j_E = D^2 j'_{E'}$ and $E = DE'$ are used. The photon flux per unit photon energy can be given by

$$N_E(T) = \frac{F_E}{E}. \quad (6)$$

The observed time is $T = t - R\mu/c$ and $T = 0$ was chosen as the time of arrival at the observer of a photon emitted at $\mu = 1$, $t = t_0$ and $R = R_0$. Thus we have $t_0 = R_0/c$ and $D|_{R=R_0} = 2\Gamma/[1 + (T/T_{ang})]$ where $T_{ang} = R_0/(2\Gamma^2 c)$. Note $\beta_\Gamma = 1 - 1/2\Gamma^2$ is used in the above derivation. Using $d\mu = cdt/R$, $dt' = dt/\Gamma$, $dR' = \Gamma dR$, and $\delta(t' - t'_0)\delta(R' - R'_0) = \delta(t - t_0)\delta(R - R_0)$, one can get

$$\begin{aligned} N_E(T) &= \frac{F_E}{E} \\ &= N_0 D^2 \begin{cases} (E'/E'_p)^{\alpha+1} & E' < E'_p \\ (E'/E'_p)^{\beta+1} & E' > E'_p \end{cases} \end{aligned} \quad (7)$$

$$= N_0 D^2 \begin{cases} (\frac{E}{DE'_p})^{\alpha+1} & E < DE'_p \\ (\frac{E}{DE'_p})^{\beta+1} & E > DE'_p \end{cases}, \quad (8)$$

where $N_0 = \Sigma'_0 R_0 c / (2D_L^2 E)$ is the normalized coefficient. One can find, from the above equation, the observed photon flux behaves as $N_E \propto (1+T/T_{ang})^{\alpha-1}$ or $N_E \propto (1+T/T_{ang})^{\beta-1}$ for a given observed photon energy E . The observed photon flux within an energy interval of $E_1 - E_2$ can be written as

$$N(T) = \int_{E_1}^{E_2} \frac{F_E}{E} dE \quad (9)$$

The decay phase of light curve in GRB is usually believed to be the result of curvature effect, i.e., the photons at higher latitude arrive at the observer more later with lower flux due to the spherical emitting area and Doppler effect. If we consider the light curve for a given observed energy, then the comoving (or intrinsic) photon energy contributing to the given observed photon energy moves toward higher energy end with the decay of light curve due to the Doppler effect. The movement would experience a break so long as the given energy is less than E_p since the intrinsic spectrum is a broken power law form. The light curve will first decay with $N_E \propto (1 + T/T_{ang})^{\alpha-1}$, and then with $N_E \propto (1 + T/T_{ang})^{\beta-1}$ so long as the given observed energy satisfies $E < E_p$. The transition time, defined as T_{ep} , is the time when the intrinsic photon energy contributing to the flux at E just moves to E'_p . However, usually the full width half maximum (FWHM, defined as $T_{1/2}$) of a pulse or the width when the flux decays to $1/e$ of peak flux (defined as $T_{1/e}$), as used in this paper, are considered to be the widths of the pulse. These artificial definitions of pulse width could lead to the result that the energy dependence of pulse width with energy does not be *measured* though it can present. The reason is as follows. Following the the definition of $T_{1/2}$, it can be given by $T_{1/2} = [2^{-1/(\alpha-1)} - 1]T_{ang}$. Consider an observed photons with energy $E < E_p$. The intrinsic contribution to it is initially from photons of $E'_a = E_a/(2\Gamma) < E'_p$. When the photon energy increase from E'_a to E'_p as the decay of Doppler factor in high

latitude region, the Doppler factor is $D_{E_a} = E_a/E'_p = 2\Gamma/(1 + T_{ep}/T_{ang})$ and the time is T_{ep} , so T_{ep} is solved to be $T_{ep} = (2\Gamma E'_p/E_a - 1)T_{ang}$. If $T_{ep} > T_{1/2}$, i.e., $\alpha < 1 - \ln 2/\ln(E_p/E_a)$, then the FWHM is only determined by the low energy section, otherwise, the FWHM of light curve will be affected by the high energy part of the intrinsic spectrum. If two photons, say E_a and E_b , both satisfy $\alpha < 1 - \ln 2/\ln[E_p/E_a(b)]$, then we can't *measured* the energy dependence of pulse width. Only if one of the photon energies or both of them satisfy the condition $\alpha > 1 - \ln 2/\ln[E_p/E_a(b)]$, the energy dependence of pulse width would be *measured*. If we consider the time $T_{1/e}$, then $T_{ep} < T_{1/e}$ gives

$$\alpha > 1 - 1/\ln(E_p/E_a). \quad (10)$$

In this condition, the closer to E_p the photon energy (i.e., the higher energy), the narrower the pulse width of this energy, shown in Figure 8. This naturally explains the energy dependence of pulse width. If two energy bands are both more energetic than E_p , then the pulse widths in these two bands will be the same, i.e., no pulse broadening with energy presents in current consideration.

BATSE bursts, the typical E_p is ~ 200 keV, the typical low energy slope is -1 and four energy channels are (25-50, 50-100, 100-300, and 300-1000 keV) (Preece et al. 2000). The condition (10) give $E_p > 121$ keV for the typical parameters. Therefor for energy channels 1 and 2, the condition is not satisfied and thus the pulse broadening in low energy band will not be measured in the two channels. However, it is so only for typical parameters. For a specific burst, $\alpha > 1 - 1/\ln(E_p/E_a)$ may be satisfied. Channel 3 crosses the typical E_p , while channel 4 is larger than it and thus only decays with $N_E \propto (1 + T/T_{ang})^{\beta-1}$. Thus the pulse width will generally decrease from energy channel 4 to channel 2. In current consideration, our results indicate no broadening measured in channels 1 and 2 for the bursts with typical parameters. However, there are two possibilities to lead to the broadening in channels 1 and 2.

One possibility is that the shell of internal shock is not a spherical symmetry, which is proposed by some authors, e.g., Fenimore & Sumner (1997) and Kocevski, Ryde & Liang (2003). Kocevski, Ryde & Liang 2003 found that only $\sim 40\%$ bursts are consistent with the spherical curvature. Their results point to a picture that the shell is a prolate geometry for a large number of bursts. In this case, the Doppler factor is decreasing faster than the spherical geometry so that the condition of (10) is easier to satisfy. Thus the prolate shell could lead to the broadening in channels 1 and 2. Another one is that the intrinsic spectrum can be evolving. If the intrinsic spectrum is evolving, e.g., E_p decreasing with time, then the condition (10) can be satisfied so that the pulses in channels 1 and 2 also broaden with energy. However, we do not know how the intrinsic spectrum evolves and how fast it does. The curvature effect naturally gives rise to an observed spectral evolution due to the Doppler effect, which gives an E_p decay with T^{-1} for a spherical curvature. If intrinsic spectral evolution gives a steeper observed one than T^{-1} , then it will be masked and thus yield to T^{-1} given by curvature effect.

The above analysis assumes the intrinsic spectrum is broken power law, so the light curve broken of decay phase at T_{ep} can be seen clearly (see Fig. 8). Actually the GRB spectrum is generally smoothly connected at the broken energy, namely, the Band spectrum, and the observed light curve is usually from an energy interval, not a single energy, so the observed decay phase is usually smooth. Note that total pulse width in GRB is dominated by decay phase. Thus the curvature effect+Band spectrum we consider here can provide a natural explanation to the energy dependence of GRB total pulse width, not only the decay width.

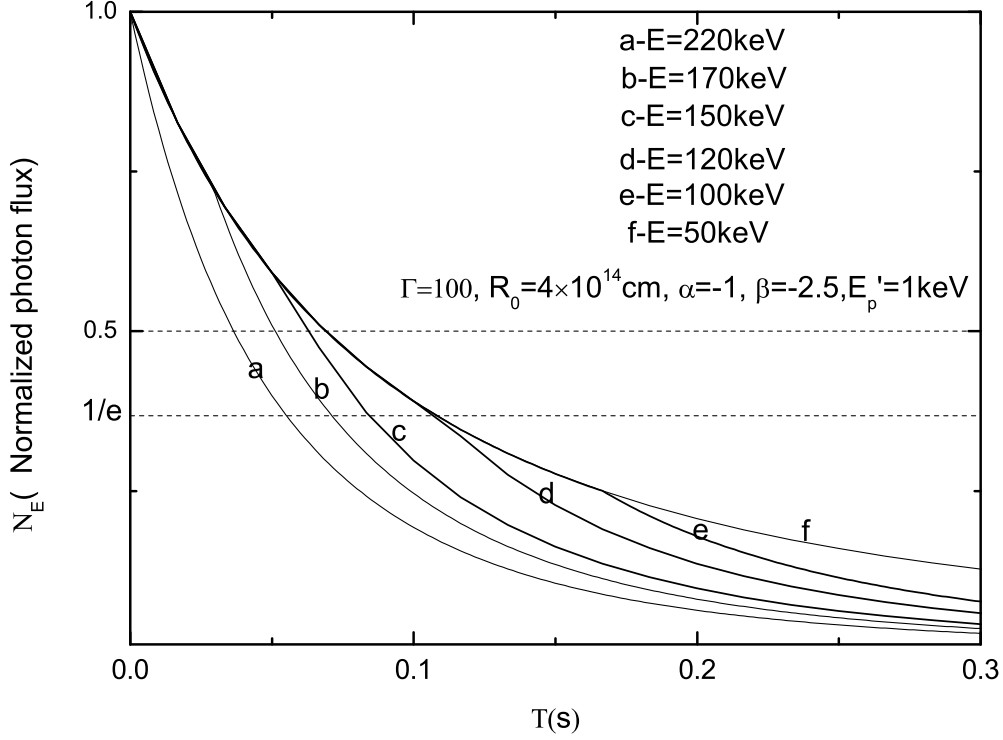


Fig. 8.— The light curves for different photon energy. Arrows mark the positions of T_{ep} . The dashed lines label the positions of half and $1/e$ maximum flux. Line a decays as $(1 + T/T_{ang})^{\beta-1}$, lines b, c, d and e first as $(1 + T/T_{ang})^{\alpha-1}$ and then as $(1 + T/T_{ang})^{\beta-1}$ and line f as $(1 + T/T_{ang})^{\alpha-1}$. Lines b and c show energy dependence of width of decay while the lines d and e do not due $T_{1/2} < T_{ep}$ if considering FWHM as the decay width.

4.2. $\delta_d - \alpha$ relation

We have shown the Band spectrum+curvature effect is a reason of pulse broadening with photon energy. Different Band function parameters will cause the differences of the degree of pulse broadening. However, the effects of the three Band function parameters, α , β and E_p , on the degree of pulse broadening are different. The main effect seems to come from the low-energy slope. The reason is the low-energy section is usually flatter than the high one, i.e., $\alpha > \beta$. Thus the decay, $N_E \propto (1 + T/T_{ang})^{\alpha-1}$, is also more shallow than $N_E \propto (1 + T/T_{ang})^{\beta-1}$ with the pulse decay width dominated by α , unless the given energy $E > E_p$. One can come to the conclusion that the larger α , the more significant the broadening with energy. Suppose two extreme cases: $\alpha = \beta$, i.e., the spectrum is a single power law; $\alpha = 1$ and $\beta = \infty$, i.e., the spectrum is composed of a horizon line and the vertical line. The pulse width would be the same for different energy bands in the former case, while the broadening of pulse with energy is the most significant in the latter case. Other cases lies between the two cases. It is difficult to find directly whether this is consistent with the observed anticorrelation in the earlier sections. We thus make a calculation to test that.

In order to compare with the observations, we calculate the count rate within four energy channels (25-50, 50-100, 100-300, and 300-1000 keV) with equation 9. Further we calculate the decay width of pulse within the four energy channels, fit linearly the width-energy relation and then find the power law slope, δ_d . Figure 9 shows our theoretically calculated $\alpha - \delta_d$ relation. Obviously, α and δ_d are roughly linearly anti-correlated, which is consistent with the statistical results of the observations. The fitted slope in Figure 9 is 0.3, also roughly consistent with the statistical results. This suggests that the curvature effect+Band spectrum could lead to the observed $\delta_d - \alpha$ correlation. Strictly speaking, δ_d and α are not linearly correlated for the theoretical results (still see Figure 9), not

completely consistent with the observations. However, in our calculations, some plausible values of the parameters, for instance the Lorentz factor and the peak energy, are used, disregarding the variety of the parameter value for different bursts, which could lead to the inconsistency. Further whether the relation in physics is linearly anti-correlated or other forms is not important. The observed relation results from the sum of intrinsic physical factors, such as the Band spectrum, curvature effect and some artificial factors, such as the energy channel selection of BATSE and the pulse width definition, which is difficult to figure out one by one. Here we only focus on the Band spectrum and curvature effect. What we concern here is the effect of the combination of them on the pulse. We find that the curvature effect+Band spectrum can indeed result in such an anti-correlated trend of $\alpha - \delta_d$.

5. Discussion and Conclusions

In this paper, we have selected 51 well-separated long-duration FRED GRB pulses from the available sample of BATSE and analyzed the pulse temporal and spectral parameters with the aim to search for their connections. Our analysis first shows that the pulse width, pulse rise width and pulse decay width with energy all scale as a power law with the power-law slopes of δ_w , δ_r and δ_d , respectively. In addition, the slopes are correlated to each other but the correlation between δ_w and δ_d is much stronger than that of δ_w and δ_r as well as δ_r and δ_d , which may be due to the pulse width is dominated by the decay phase and the rise and decay phase have different origins.

Then we investigate the relations between the power-law indices and the three Band spectral parameters. Our results show that the power-law indices, δ_w , δ_d are strongly correlated with the low-energy index α and much less correlated with high energy slope β . The δ_r weakly correlates with β but does not show apparent correlated with α .

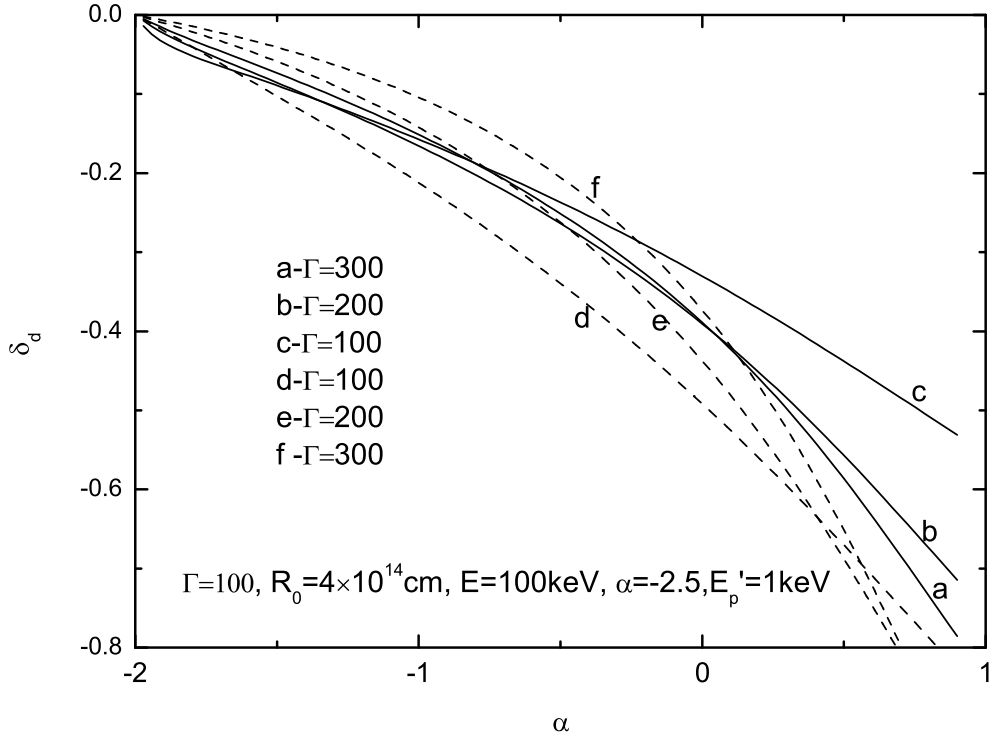


Fig. 9.— $\delta_d - \alpha$ relation. The solid lines are for 4 channels of BATSE considered, while the dashed lines for 1, 2 and 3 channels case. The latter is considered due to the fact that the fitted δ_r , δ_d and δ_w in statistical part of the paper are obtained mainly using channels 1, 2 and 3.

We do not find that there are apparent correlated relations between the peak energy E_p and three power-law indices based on our current sample (see, Figure 7 and Table 4). However, we think the demonstrations that δ_w , δ_r , and δ_d are independent of E_p may be weak only based on our current sample. Several reasons may cause the case. Firstly, it is well known that the BATSE E_p distribution is narrow (e.g. Band et al. 1993, Mallozzi et al. 1995, Schafer 2003), and thus it can be hard to clearly identify the correlations in data drawn from a narrow distribution. Secondly, the sample is likely biased toward low E_p -valued pulses. The sampled pulses have been selected on the basis of long durations and bright peak fluxes. Because of pulse property correlations, such pulses tend to be softer than the mean (Hakkila and Preece, 2011). This pulse selection bias can have contributed to the narrowness of the sample. Lastly, some of the highest E_p pulses in this sample may have been incorrectly identified as single pulses, when in actuality they represent merged pulses. If the hard-to-soft pulse evolution demonstrated by Peng et al. (2009a) is normal, then a pulse made from two merged pulsed will experience a re-hardening when the second pulse kicks in (Hakkila and Preece 2011; Ukwatta 2011), which can give these pulses higher E_p values than the other single pulses to which they are being compared. Due to the bad fits to those merged pulses with given pulse model we are not sure how the merging of pulses affects the δ values from the data analysis. But we can give some reasonable deductions. Firstly, it seems that the smallest δ value from a merged pulse occurs when pulses overlap completely (i.e. when they peak at the same time). Otherwise, the pulses should appear to be longer in all energy channels, and the pulse separation will make a larger contribution to the pulse broadening than the energy-dependent broadening embedded within it. Secondly, we find that the correlations between E_p and δ_s are still positive and the correlations get much weaker after removing those merged pulses with high E_p values. Therefore, if the merged pulses can cause high E_p and the positive correlations between E_p and δ_s indeed exist the overlapping pulses may also make the δ_s small. Based on the above analysis we

think the merged pulses would make the δ values decrease. In order to identify further the correlations between E_p and δ s more wider energy band and cleaner single pulse data are needed.

We further investigate the implications of the statistical relations. We find that the energy dependence of decay width (also the pulse width since it is dominated by the decay section) can be caused by the curvature effect+Band spectrum. Usually we study the observed light curve for a given energy or energy interval (e.g., BATSE has 4 energy channels). The light curve decays due to the delay arrival of high-latitude photons with lower flux, i.e., curvature effect. For a given observed energy less than the peak energy of Band spectrum, the intrinsic photon energy contributing to the energy will move from low energy part of Band spectrum to high energy one due to the lower Doppler factor at high latitude. This will naturally lead to the energy dependence of decay width and thus the pulse width. This in turn supports the decay phase is indeed due to the curvature effect, or at least related to it. In addition, different Band function parameters may lead to the different degree of pulse broadening. The main effect seems to be from the low-energy slope as analyzed above. The strong correlation between δ_d and α also appears to result from the curvature effect and Band spectrum (see Fig.9).

The rise phase of the GRB pulse contributes less to the pulse width than the decay phase. However it is important and is considered to be relevant to the hydrodynamic time of shock crossing shell. Statistical studies have found that the rise phase is also related to the time-resolved Band spectrum in single pulse. For instance, some authors found that the time-resolved peak energy of pulse is tracking the pulse profile within a pulse for some bursts (Kaneko et al. 2006; Peng et al. 2009b, however, see Hakkila & Preece 2011 for different view). In current investigations, we didn't find correlations between broadening of the rise phase and the (time-integrated) Band spectrum parameters for different pulses,

suggesting that the formation of the rise phase is related to emission mechanism, while its energy dependence is independent of emission mechanism. The energy dependence of rise phase may arise from the intrinsic spectral evolution. As pointed by Fenimore & Sumner (1997), the intrinsic spectral evolution affects the rise phase much more significant than the decay phase.

A deduction of the correlation between δ_d and α we found is that the energy dependence of pulse with single power law (corresponding to $\alpha = \beta$ in Band spectrum) spectrum is systematically weaker than that with Band spectrum. If it is verified, this will support that the intrinsic Band spectrum and the curvature effect is indeed an important factor leading to the photon energy dependence of GRB pulses. Also it in turn supports that the decay phase of pulse is produced by the curvature effect. We will consider it in a future paper with Fermi/GBM or Konus-Wind data.

6. Acknowledgments

We thank the anonymous referee for constructive suggestions. This work was supported by the Natural Science Fund of Yunnan Province (2009ZC060M), the Key Program for Science Fund of the Education Department of Yunnan Province (2011Z004), the Open Research Program of Key Laboratory for the Structure and Evolution of Celestial Objects (OP201106), and the National Natural Science Foundation of China (no. 10778726).

REFERENCES

- Band, D., et al. 1993, ApJ, 413, 281
- Band, D., 1997, ApJ, 486, 928
- Chiang, J., 1998, ApJ, 508, 752
- Chincarini, G. et al., 2010, MNRAS, 406, 2113
- Crew, G. B. et al., 2003, ApJ, 599, 387
- Crider, A., et al. 1997, ApJ, 479, L39
- Dermer, C. D., 1998, ApJ, 501, L157
- Fenimore, E. E., et al. 1995, ApJ, 448, L101
- Fenimore, E. E., & Sumner 1997, arXiv:astro-ph/9705052
- Fenimore, E. E., et al. 1999, ApJ, 518, 375
- Hakkila, J., Giblin, T. W., Norris, J. P., Fragile, P. C., Bonnell, J. T. 2008, ApJ, 677, L81
- Hakkila, J., & Preece, R. D. 2011, ApJ, 740, 104
- Kaneko, Y., et al. 2006, ApJS, 166, 298
- Kazanas, D., Titarchuk L. G., Hua X.-M., 1998, ApJ, 493, 708
- Kocevski, D., Ryde, F., & Liang, E. 2003, ApJ, 596, 389
- Kocevski, D., & Liang, E. 2003, ApJ, 594, 385
- Link B., Epstein R. I., Priedhorsky W. C., 1993, ApJ, 408, L81
- Mallozzi, R. S., et al. 1995, ApJ, 454, 597

Nemiroff, R. J., 2000, ApJ, 544, 805

Norris, J. P., et al. 1996, ApJ, 459, 393

Norris, J. P., Marani G. F., Bonnell J. T., 2000, ApJ, 534, 248

Norris, J. P., et al. 2005, ApJ, 627, 324

Peng, Z. Y., et al. 2006, MNRAS, 368, 1351

Peng, Z. Y., et al. 2007, ChjAA, 7, 428

Peng, Z. Y., et al. 2009a, ApJ, 698, 417

Peng, Z. Y., et al. 2009b, NewA, 14, 311

Peng, Z. Y., et al. 2010, ApJ, 718, 894

Qin, Y. P., Dong Y. M., Lu R. J., Zhang B. B., Jia L. W., 2005, ApJ, 632, 1008

Schaefer, B. E., 2003, ApJ, 583, L71

Shen, R. F., Song, L. M., Li, Z., 2005, MNRAS, 362, 59

Ukwatta, T. N., et al. 2011, MNRAS, 412, 875

Wang, J. C., Cen X. F., Qian T. L., Xu J., Wang C. Y., 2000, ApJ, 532, 267

Zhang, F. W., Qin, Y. P., & Zhang, B. B., 2007, PASJ, 59, 857

Zhang, F. W., & Qin, Y. P., 2008, NewA, 13, 485

Zhang, F. W., 2008, ApJ, 685, 1052